JPP JOURNAL OF Pharmacy and Pharmacology
ROYAL PHARMACEUTICAL SOCIETY
JPP Journal of Pharmacy And Pharmacology
Research Paper

Synthesis, characterization, antidiabetic and antioxidative evaluation of a novel Zn(II)-gallic acid complex with multi-facet activity

Denice M. Motloung[a], Samson S. Mashele[a], Godfrey R. Matowane[a], Shasank S. Swain[b], Susanna L. Bonnet[c], Anwar E.M. Noreljaleel[c], Sunday O. Oyedemi[d] and Chika I. Chukwuma[a]

[a]Department of Health Sciences, Faculty of Health and Environmental Sciences, Central University of Technology, Bloemfontein, Free State, South Africa, [b]Division of Microbiology and NCDs, ICMR-Regional Medical Research Centre, Bhubaneswar, Odisha, India, [c]Department of Chemistry, Faculty of Natural and Agricultural Sciences, University of the Free State, Bloemfontein, South Africa and [d]Department of Biochemistry, Michael Okpara University of Agriculture, Umudike, Nigeria

Keywords
diabetes; gallic acid; glucose uptake; zinc(II) acetate; Zn(II) complex

Correspondence
Chika I. Chukwuma, Department of Health Sciences, Faculty of Health and Environmental Sciences, Central University of Technology, Private Bag X20539, Bloemfontein 9300, Free State, South Africa.
E-mails: chykochi@yahoo.com; cchukwuma@cut.ac.za

Received March 16, 2020
Accepted May 30, 2020

doi: 10.1111/jphp.13322

Abstract

Objectives This study was done to synthesize a novel Zn(II)-gallic acid complex with improved antidiabetic and antioxidative properties.
Methods The complex was synthesized and characterized using Fourier Transform Infrared (FT-IR) and ^{1}H NMR. Cytotoxicity was evaluated using Chang liver cells and L6 myotubes. Radical scavenging and Fe^{3+}-reducing, as well as α-glucosidase, α-amylase and glycation inhibitory properties were measured. Glucose uptake was measured in L6 myotubes, while the complex was docked against glucose transporter type 4 (GLUT-4) and protein kinase B (PKB).
Key findings Analysis showed that complexation occurred through a $Zn(O_4)$ coordination; thus, the complex acquired two moieties of gallic acid, which suggests why complexation increased the DPPH (IC_{50} = 48.2 μM) and ABTS (IC_{50} = 12.7 μM) scavenging and α-glucosidase inhibitory (IC_{50} = 58.5 μM) properties of gallic acid by several folds (5.5, 3.6 and 2.7 folds; IC_{50} = 8.79, 3.51 and 21.5 μM, respectively). Zn(II) conferred a potent dose-dependent glucose uptake activity (EC_{50} = 9.17 μM) on gallic acid, without reducing the viability of L6 myotubes and hepatocytes. Docking analysis showed the complex had stronger interaction with insulin signalling proteins (GLUT-4 and PKB) than its precursor.
Conclusions Data suggest that complexation of Zn(II) with gallic acid resulted in a complex with improved and multi-facet antioxidative and glycaemic control properties.

Introduction

Diabetes mellitus (DM) is a group of metabolic diseases characterized by hyperglycaemia resulting from defects in insulin secretion, insulin action or both.[1] Its global prevalence has been reported to be 425 million people, which is expected to increase by 48% by 2045.[2] Type 1 diabetes is characterized by loss of pancreatic insulin secretion, predominantly due to autoimmune pancreatic ß-cell destruction.[1] Type 2 diabetes (T2D), which is the most prevalent type of diabetes (about 90% of cases), is caused by insulin insensitivity in target tissues accompanied by partial ß-cell dysfunction.[3]

Insulin resistance in T2D leads to impaired glucose uptake in peripheral tissues and uncontrolled hepatic glucose output, which contributes to persistent hyperglycaemia.[4] Persistent hyperglycaemia is responsible for several microvascular and macrovascular complications associated with T2D. Oxidative stress is a major mediator in the development and progression of diabetic complications, due to the elevation of pro-oxidants production during diabetes, which oxidatively damage biological molecules, cells, tissues and organs, thus leading to diabetic complications.[5]

Despite numerous synthetic and commercial antidiabetic drugs, most of them are not affordable to a large portion of

the diabetic population and some of them pose short- and long-term side effects.[6] Thus, the search for more effective and safer hypoglycaemic agents remains an important area of research.

Advances in antidiabetic drug discovery suggest that mineral supplements may be promising targets for the development of potent antidiabetic agents.[7,8] This is because they function as essential coenzymes and cofactors for metabolic processes that maintain normal glucose, lipid and protein metabolism, while pharmacological studies have given credence to their modulatory effects on glucose and lipid metabolism in diabetes, obesity and related metabolic diseases.[9] Particularly, Zn(II) has been reported to show relatively high insulin-mimetic properties with less toxicity compared with other metal elements.[10,11] Zn(II) stimulates both lipogenesis and glucose transport in adipocytes.[12,13] In human and mouse skeletal muscle cells, Zn (II) modulated insulin signalling, which resulted in enhanced glucose oxidation and glycaemic control[14] and thus could be a potential target for the development of a therapeutic agent for diabetes.

On the other hand, plant-derived phenolic acids have been reported to be partly responsible for the antidiabetic and antioxidative properties of many plants.[15] Gallic acid is a well-known natural antioxidant present in plants. It scavenges reactive oxygen species (ROS), including superoxide anions, hydrogen peroxide, hydroxyl radicals and hypochlorous acid, thus attenuating oxidative stress.[16] Additionally, several studies reported in a previous review[17] showed that gallic acid decreased hyperglycaemia and acutely improved insulin sensitivity. It increased GLUT-4 activity and insulin sensitivity through PPAR-γ and Akt signalling in 3T3-L1 preadipocytes and modulated glucose homeostasis and insulin sensitivity in db/db mice and fructose-fed rats.[18] Also, it exhibited inhibitory activities on α-glucosidase and α-amylase activities, as well as Fe^{2+}-induced lipid peroxidation.[19] Furthermore, the effects of gallic acid on several biochemical and histopathological parameters in streptozotocin-induced diabetic rats suggested a cardioprotective action of gallic acid, which may be attributed to its concomitant, antihyperglycemic, anti-lipid peroxidative and antioxidant effects.[20]

Furthermore, growing evidence indicate that polyphenols coupled with zinc mineral may help control and prevent diabetes complications, making it a potential adjuvant for antidiabetic phenolics. In fact, several studies consistently showed that Zn(II) complexes of some plant-derived flavonoids positively influenced glycaemic control, antioxidant status and lipid profile.[21-24] In spite of the possible improvement of the antidiabetic efficacy of gallic acid by complexing Zn(II), the study has not been undertaken, leaving a scientific gap in this area of research. Therefore, this study was done to synthesize, characterize and evaluate the antidiabetic and antioxidative properties of a novel with Zn(II)-gallic acid complex.

Materials and Methods

Synthesis of Zn(II) complex of gallic acid

Complex was be synthesized from Zn(II) acetate dihydrate and gallic acid in a 1 : 2 mole ratio, respectively, using a previous method[25] with some modifications. Both Zn(II) acetate dihydrate and gallic acid monohydrate were purchased from Sigma Aldrich (Johannesburg, South Africa). Briefly, 376.3 mg of gallic acid monohydrate (Mr = 188.13 g/mol) and 219.51 mg Zn(II) acetate dihydrate (Mr = 219.51 g/mol) were each separately dissolved in 5 ml of methanol. Thereafter, both solutions were gradually mixed, while stirring. The complex was formed as a white/milky gelatinous precipitate, which was recovered by filtration. The precipitate was washed three times with 50% (v/v) methanol, dried and stored at room temperature in air-tight glass vials.

FTIR analysis of complex

The FT-IR spectrometer (Perkin Elmer Spectrum 100 FTIR Spectrometer, Waltham, MA, USA) was used to analyse the infrared spectrum of the complex using an ART accessory. Analysis was done at a scan rate of 40 per second in the range of 4000–380 cm^{-1}. The crystal of the sample holder of the equipment was loaded with about 1 mg of sample to cover it. The arm of the instrument was then lowered, and the sample was scanned to obtain the IR spectrum.

Proton NMR (^{1}H NMR) analysis of complex

A 600 MHz Bruker Avance™ spectrometer (Bruker Corporation, Billerica, MA, USA) was used to record the ^{1}H NMR in **DMSO**-d_6 (δH = 2.50), with tetramethylsilane as internal standard. Chemical shifts were expressed as parts per million (ppm) on the delta (δ) scale and coupling constants (J) are accurate to 0.01 Hz.

Cytotoxicity evaluation of complex

The effect of the complex on cell growth or viability was done on Chang liver cell lines using standard MTT [3-(4,5-dimethylthiazol-2-yl)-2,5-diphenyltetrazolium bromide] assay. Human Chang liver cells (ATCC CCL-13™, American Type Culture Collection, Manassas, VA, USA) were seeded in 100 µl medium in 96-well plates at a concentration of 1 × 105 cells/ml and incubated for 24 h humidified CO2 incubator (NÜVE EC 160, Ankara, Turkey) set at 5% CO_2, 95% oxygen and 37°C to allow cells to attach to the

bottom of the wells. Thereafter, used medium was replaced with 100 µl of fresh culture medium containing different concentrations (8.4, 84 and 840 µM in final assay volume) of complex and not more than 0.5% DMSO. Controls included cells exposed to 0.5% DMSO. After the 36 h treatment period, 100 µl (0.5 mg/ml in final volume) of MTT reagent (Sigma Aldrich) was added to wells, the plate was swirled gently to mix content and incubation continued for 3 h. Thereafter, wells were aspirated, and cells were washed with 100 µl of phosphate-buffered saline (PBS). A 100 µl of MTT de-staining or solubilization solution was added, and absorbance was measured using a plate reader (Multiskan Go, Thermo Fischer Scientific, Waltham, MA, USA) at 570 nm wavelength. Media-sample blank was included and used to normalize the results. The samples were evaluated in two independent biological repeats, and each sample was evaluated in triplicate for each biological repeat. The cell growth/viability inhibition was computed using the following formula:

$$\text{Cell growth inhibition}\,(\%) = \frac{\text{Absorbance of control} - \text{Absorbance of test}}{\text{Absorbance of control}} \times 100$$

2,2-diphenyl-1-picrylhydrazyl (DPPH) radical scavenging activity

A previous method[26] with slight modification was used to measure the DPPH scavenging activity of the complex. The assay mixture contained 75 µl different concentrations (3.75–60 µM in reaction mixture) of the complex, its precursor gallic acid, zinc(II) acetate or standards (ascorbic acid and Trolox) or their solvents (control) and 37.5 µl of a 0.3 mM DPPH solution in a 96-well plate. The mixture was incubated in the dark for 30 min, and absorbance was measured at 517 nm (SpectraMax M2 microplate reader, Molecular Devices, San Jose, CA, USA). Sample blank or sample solvent was used as the blank. The formula below was used to calculate the DPPH radical scavenging activity (%):

$$\text{Scavenging activity}\,(\%) = \frac{\text{Absorbance of control} - \text{Absorbance of test}}{\text{Absorbance of control}} \times 100$$

ABTS [2,2′-Azino-bis(3-ethylbenzothiazoline-6-sulfonic acid) diammonium salt] radical scavenging activity

The method reported by Re et al.[27] as modified by Oyedemi et al.[28] was used to measure this property of the complex and its precursor. ABTS radical was generated by equally mixing 7 mM ABTS and 2.4 mM potassium persulphate solutions and incubating the mixed solutions at room temperature in the dark for 12–16 h. The solution was then diluted with methanol until an absorbance of 0.706 at 734 nm was attained. The assay was performed as follows: 50 µl of different concentrations (3.75–60 µM in reaction mixture) of the complex, its precursor gallic acid, zinc(II) acetate or standards (ascorbic acid and Trolox) or their solvents (control) were mixed with 125 µl of the diluted ABTS solution in a 96-well plate. Absorbance at 734 nm was measured after a 15 min incubation in the dark. The following formula was used to compute the ABTS radical scavenging activity (%) of test samples:

$$\text{Scavenging activity}\,(\%) = \frac{\text{Absorbance of control} - \text{Absorbance of test}}{\text{Absorbance of control}} \times 100$$

Fe^{3+} reducing antioxidant power

A method slightly modified from a previous method[26] was used to measure the Fe^{3+} reducing antioxidant power (FRAP) of complex. First, 25 µl each of complex, its precursor gallic acid, zinc(II) acetate, Trolox (at 40 µM in reaction mixture) or ascorbic acid standards (4–80 µM in reaction mixture), 0.2 M phosphate buffer (pH 6.6) and 1% potassium ferricyanide were mixed and incubated for 20 min at 50°C. The mixture was acidified with 25 µl of 10% TCA, and then 100 µl of distilled water and 50 µl of 0.1% $FeCl_3$ solution were added, successively. Absorbance was then measured at 700 nm and the FRAP of the complex, its precursor gallic acid, zinc(II) acetate and Trolox (positive control) was determined from ascorbic acid standard curve and computed as mmol/mol equivalent of the standard using the following formula:

$$\text{FRAP}(\text{mmol/mol AAE}) = \frac{C \times \text{SV}}{M}$$

where, 'C' is the concentration (mmol/ml) extrapolated from ascorbic acid standard curve; 'SV' is the sample volume (ml), and 'M' is the amount (mole) of the sample in SV (ml) of the sample solution; 'AAE' means 'ascorbic acid equivalent'.

Glycation inhibition

The protein glycation inhibitory effect of the complex and its precursor was measured using a previous method[29] with some modifications.[30] Briefly 50 µl volume of different concentrations (3.75–60 µM in reaction mixture) of the samples or standard (aminoguanidine) or their solvents (control) was incubated with 50 µl of glucose (90 mg/ml)

and 50 µl bovine serum albumin (10 mg/ml) in the dark for 3 weeks at 37°C using black 96-well plates. Thereafter, fluorescence was measured at Ex/Em = 360 nm/420 nm, and the glycation inhibition was computed using the following formula:

$$\text{Glycation inhibition}\,(\%) = \frac{\text{Fluorescence of control} - \text{Fluorescence of test}}{\text{Fluorescence of control}} \times 100$$

α-amylase inhibition

The methods reported by Sanni et al.[26] was used to measure the enzyme inhibition. In a 2 ml vial, 75 µl of different concentrations (5–80 µM) of samples or standard (Acarbose) or their solvents (control) was mixed with 75 µl of 3 U/ml porcine pancreatic amylase (Sigma Aldrich) solution (dissolved in 100 mM phosphate buffer, pH 6.8) and incubated at 37°C for 15 min. Equivalent volume of 1% starch (dissolved in 100 mM phosphate buffer, pH 6.8) was then added and incubation continued for 30 min at 37°C. Thereafter, 75 µl of dinitrosalicylate (DNS) colour reagent was added and the mixture was boiled for 10 min. After cooling, each vial was centrifuged (5 min at 2370 *g*; Hettich Mikro 200 microcentrifuge, Hettich Lab Technology, Tuttlingen, Germany) and a 150 µl aliquot of supernatant was transferred into a 96-well plate and absorbance was then read at 540 nm. The enzyme inhibition (%) of the samples was computed using the following formula:

$$\text{Enzyme inhibition}\,(\%) = \frac{\text{Absorbance of control} - \text{Absorbance of test}}{\text{Absorbance of control}} \times 100$$

α-glucosidase inhibition

The α-glucosidase inhibitory potential of the complex was measured using a previous method[26] with slight modification. To perform this assay, 25 µl of different concentrations (3.75–60 µM in reaction mixture) of samples or standard (acarbose) or their solvent (control) was mixed with 50 µl of 2 U/ml α-Glucosidase from rice (Sigma Aldrich) solution (dissolved in 100 mM phosphate buffer, pH 6.8) in a 96-well plate and incubated at 37°C for 10 min. A 25 µl of 5 mM pNPG (dissolved in 100 mM phosphate buffer, pH 6.8) was then added and the mixture was further incubated for 20–30 min at 37°C. Thereafter, 100 µl of 100 mM Na_2CO_3 was added to stop the enzyme reaction and absorbance was measured at 405 nm. The enzyme inhibition (%) of the samples was computed using the following formula:

$$\text{Enzyme inhibition}\,(\%) = \frac{\text{Absorbance of control} - \text{Absorbance of test}}{\text{Absorbance of control}} \times 100$$

Glucose uptake in Muscle cells

Assays were performed using previously reported methods[31,32] with some modifications. L6 myoblast cells from rat muscle (ATCC CRL-1458™, American Type Culture Collection, Manassas, VA, USA) were grown in DMEM (low glucose) supplemented with 10% FCS and sub-cultured by trypsinization. Cells were seeded at a density of 5000 cells/well in 96-plate well at volumes of 200 µl/well of growth medium and incubated in a CO_2 incubator at 5% CO_2, 95% oxygen and 37°C. When approximately 80% confluent the medium was replaced with differentiation medium (DMEM containing 2% horse serum). Cells are incubated for an additional 5 days to allow enough time for full differentiation. Spent culture medium was removed from differentiated cells and replaced with fresh medium containing different concentrations (5, 37 and 50 µg/ml in 200 µl/well volume of medium) of samples or their solvent (control). Treatment continued for 48 h and thereafter, spent culture medium was removed and the cells were washed once with PBS. Immediately, 100 µl of RPMI medium supplemented with 0.1% BSA and containing 8 mM glucose was added to wells and incubated for 2 h. Positive control group also contained 1 µg/ml insulin. After 2 h of incubation at 37°C, aliquot from each well was used to measure glucose concentration (µM) using the Glucose (GO) Assay Kit (Sigma Aldrich) according to the kit protocol manual. The effect of the complex on cell viability was, also, measured using MTT assay. Assay was performed in three replicates of two biological repeats. Glucose uptake of test was computed relative to the control using the following formula:

$$\text{Glucose uptake}\,(\%) = \frac{\Delta\text{GC of test} - \Delta\text{GC of control}}{\Delta\text{GC of test}} \times 100.$$

where 'ΔGC' means change in glucose concentration (i.e. initial – final glucose concentration in incubation solutions). The EC_{50} (concentration in µM required to cause 50% glucose uptake effect) of the samples was computed and expressed in µM using on the molecular masses of the samples.

Molecular docking against GLUT-4 and PKB

The whole bioinformatics work was carried out in the Linux-Ubuntu environment. The desired chemical structure of gallic acid and gallic acid-Zn-gallic acid complex was designed by ChemDraw Ultra software and save in (.pdb)

file formats for use in molecular docking study. Due to the unavailability of the 3D structure of the targeted enzyme glucose transporter type 4 (GLUT4), a theoretical three-dimensional protein structure was modelled. Additionally, the protein kinase B (PKB) was retrieved from protein data bank with ID_106L but again remodelled for make up the slitting and gaps in retrieved 3D protein structure. The SWISS-MODEL tool was used for the modelling and remodelling of both target enzymes and check the quality, consistency and stability of the generated GLUT4 protein structure through the well-recognized Ramachandran plot before docking study.[33,34] The AutoDock 4.0 software (Scripps Research Institute, San Diego, CA, USA) for a molecular docking study and molecular interaction visualization BIOVIA-DSV was used in the present study.[33]

Statistical analysis and potency ratios

Data were analysed using Microsoft (2016) Excel or GraphPad Prism 5 (Windows version, GarphPad Softwre, San Diego, CA, USA) and presented as mean ± standard deviation of replicates. Statistical analysis was done using the IBM SPSS for Windows, version 23.0 (IBM Corp, Armonk, NY, USA) by the Tukey's multiple range post hoc tests (multiple comparison) using the one-way analysis of variance (ANOVA) for comparing the means multiple samples and significant difference between comparisons was set at $P < 0.05$.

To ascertain the extent to which Zn(II) influenced the properties of its ligands or the efficacy of the synthesized Zn(II) complex, the antidiabetic and antioxidative potency ratio (ψ) of the complex relative to the different controls (the precursor phenolic acid (PA), zinc(II) acetate (ZA) and standards: acarbose (AC), ascorbic acid (AA), Trolox (TR), aminoguanidine (AG) and insulin (IN)) was computed as follows:

$$\psi = \frac{\text{Activity of complex}(\%)}{\text{Activity of contol}(\%)}$$

$$\text{or } \left(\frac{\text{IC}_{50}\text{of complex}}{\text{IC}_{50}\text{of control}}\right)^{-1} \text{or } \left(\frac{\text{EC}_{50}\text{of complex}}{\text{EC}_{50}\text{of control}}\right)^{-1}$$

where, IC_{50} is the concentration required to cause 50% inhibition of the activities of carbohydrate digesting enzymes or 50% radical scavenging activity, while EC_{50} is the concentration required to cause 50% glucose uptake increase in L6-myotubes, which were calculated using Microsoft (2016) Excel or GraphPad Prism 5.

Results

The appearance if the synthesized complex was a white gelatinous precipitate, which turned slightly dark upon drying and is slightly soluble in DMSO. The IR spectroscopy interpretation was adopted from previous studies.[35-37] The phenolic -O-H stretching vibration peaks (broad) involved in intramolecular hydrogen bonding were observed in the FTIR absorption spectrum of gallic acid and complex in the range of 3200–3400 cm^{-1} (Figure 2) due to the presence of phenolic -OH group in gallic acid and its complex (Figure 1). This is further confirmed by the weak to medium phenolic -OH bend observed in gallic acid (1378 and 1306 cm^{-1}) and its complex (1374, 1336 and 1307 cm^{-1}) (Figure 2). However, the carboxylic -O-H stretch observed in the IR absorption spectrum of gallic acid in the range of 3263–2656 cm^{-1} (Figure 2a) was diminished in that of its complex (Figure 2b) suggesting that the carboxylic group of the phenolic acid was involved in Zn(II)-gallic acid complexation (Figure 1b). Additionally, the carboxylic -OH bend observed in the IR absorption spectrum of gallic acid as weak to medium peaks in the range of 1489–1378 cm^{-1} (Figure 2a) disappeared in the IR absorption spectrum of its complex (Figure 2b), which further supports the involvement of gallic acid's carboxylic group in complexation (Figure 1b). The peaks at 1694 cm^{-1} (Figure 2a) and 1693 cm^{-1} (Figure 2b) indicate carboxylic acid -C = O stretching, while the peaks at 1240 and 1200 cm^{-1} (Figure 2a), as well as 1236 and 1203 cm^{-1} (Figure 2b) indicates sp2 -C-O stretch of the carboxylic group of both gallic acid and its complex.

The ^{1}H-NMR spectrum of Gallic acid-zinc acetate complex represents a singlet peak at δ 6.91 characteristic of H-2/6 of the aromatic ring. Observation of H-2 and H-6 in same δ value (Figure 3 and Table 1) indicated the complex occurred by carboxylic group and not the phenolic group, which is supposed to give different environment of the two protons H-2 and H-6. Also, disappearance of the peak of the carboxylic group at δ 12.2 and the observation of the peak of the hydroxyl group at δ 9.16 (Figure 3 and Table 1) further indicates that the coordination/complexation occurred by carboxylic group. The singlet peak corresponding to the two methyl groups of the zinc acetate at δ 1.90 and the value of the integral may be affected by base line of the NMR. Based on the ^{1}H-NMR data, it was proposed that 2 molecules of gallic acid complexed with Zn(II) using a Zn (O_4) coordination mode as shown Figure 1b.

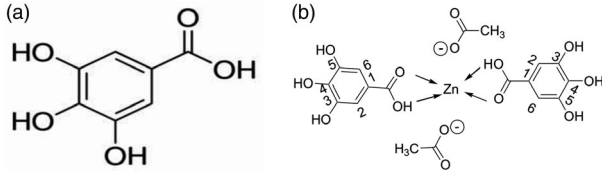

Figure 1 (a) Structure of gallic acid and (b) proposed structure of gallic acid-zinc acetate complex.

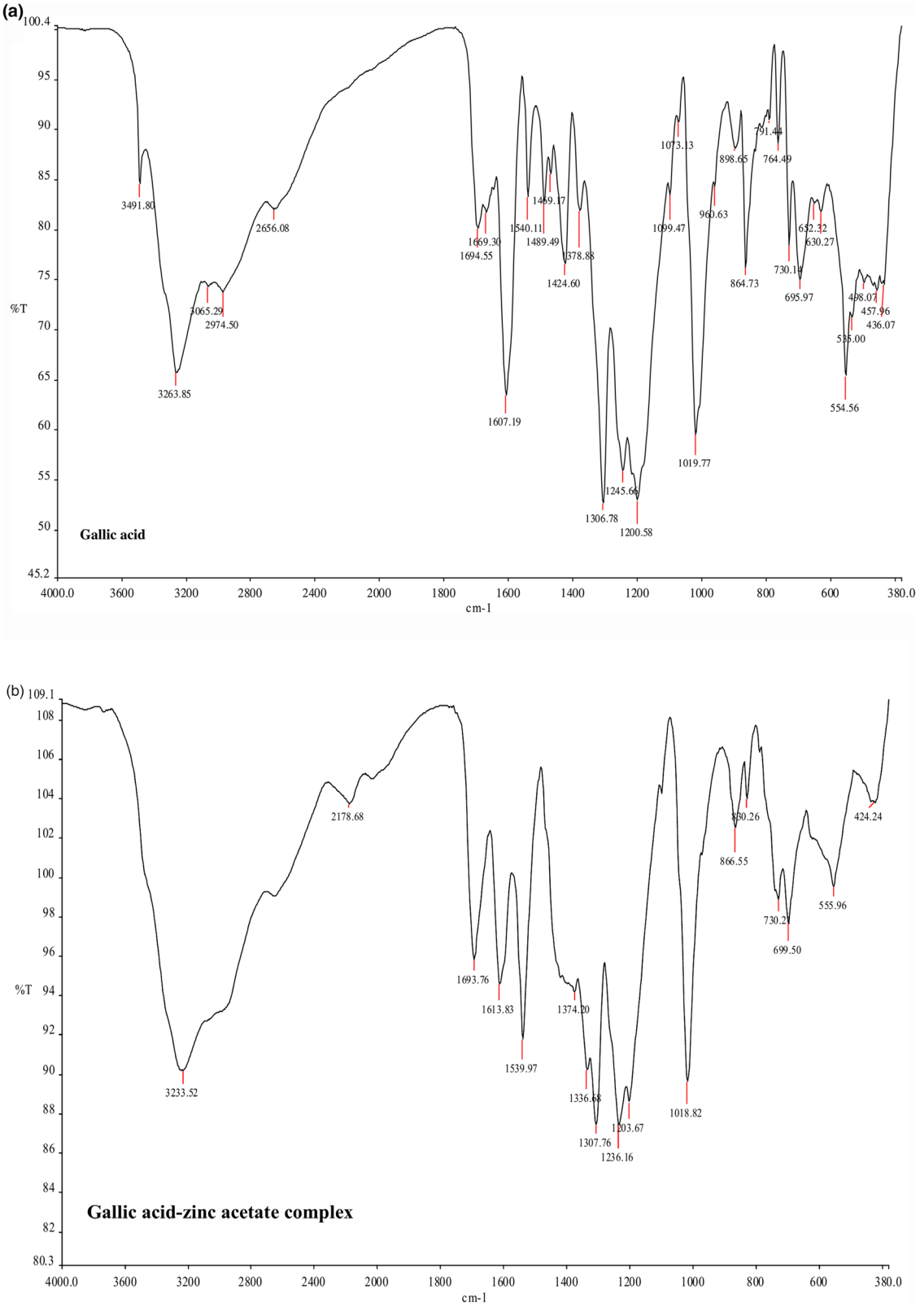

Figure 2 FT-IR spectra of (a) gallic acid and (b) gallic acid-zinc acetate complex. [Colour figure can be viewed at wileyonlinelibrary.com]

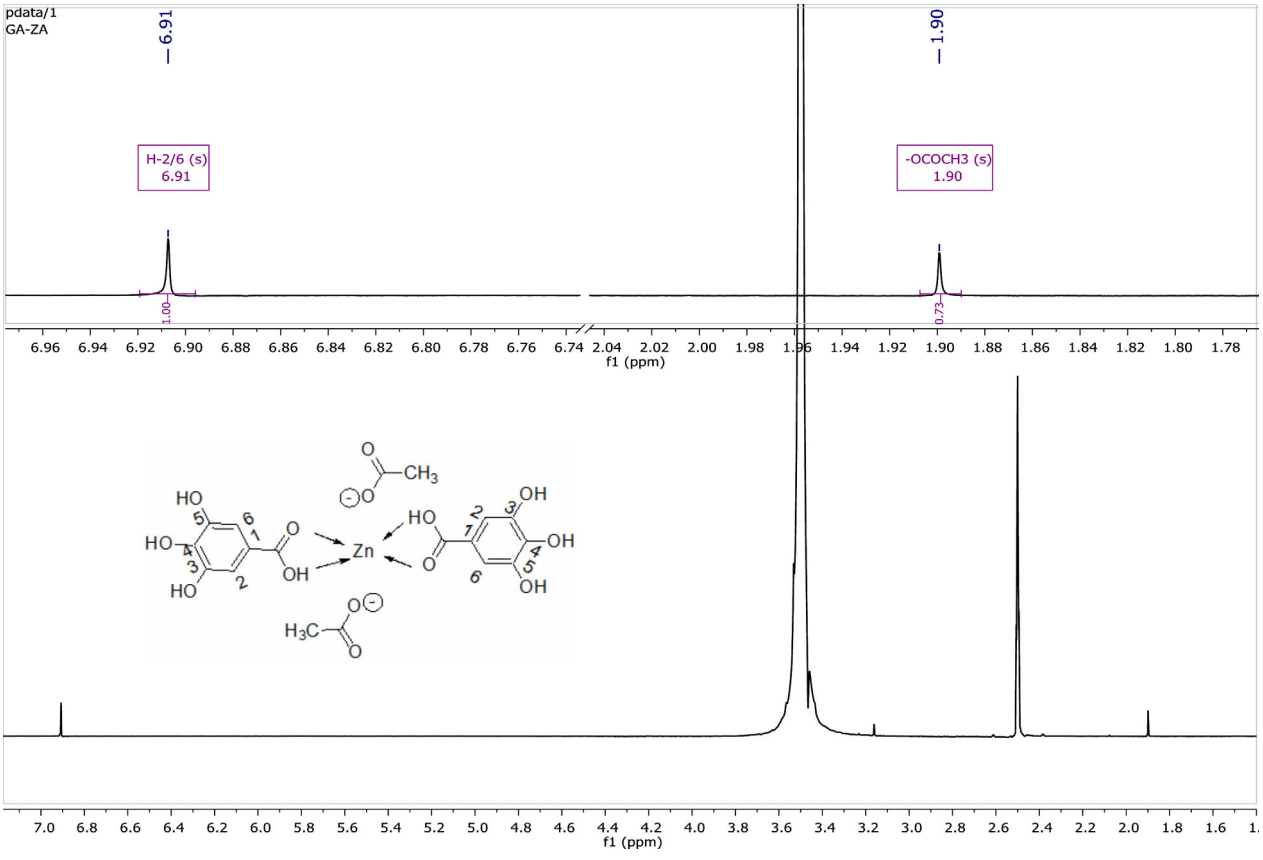

Figure 3 ^{1}H-NMR spectrum of gallic acid-Zinc acetate complex. ^{1}H NMR (600 MHz, DMSO-d_6) δ 7.45 (d, J = 7.7 Hz, 4H, H-2/6), 7.32 (t, J = 7.5 Hz, 4H, H-3/5), 7.24 (t, J = 7.3 Hz, 2H, H-4), 7.06 (d, J = 16.0 Hz, 2H, H-α), 6.35 (d, J = 15.9 Hz, 1H, H-), 1.58 (d, J = 0.9 Hz, 6H, 2CH3COO). Proposed molecular mass of complex = 477.8 g/mol. [Colour figure can be viewed at wileyonlinelibrary.com]

Table 1 ^{1}H NMR interpretation of gallic acid-zinc acetate complex

Position	^{1}H NMR (400 MHz, DMSO-d_6) δ	
1	–	–
2	6.91	2H, s
3	–	–
4	–	–
5		–
6	6.91	2H, s
-OH	9.16	9.16
CH_3COO	1.90	6H, s

Although the α-glucosidase inhibitory activity of Zn(II)-gallic acid complex (IC_{50} = 21.5 μM) was not as potent as acarbose (IC_{50} = 9.08 μM; Ψ = 0.4_{AC}), Zn(II) complexation with gallic acid increased the enzyme dose-dependent inhibitory activity of gallic acid (IC_{50} = 58.5 μM) by 2.7 folds (Ψ = 2.7_{PA}) (Figure 4a and Table 2). The α-amylase inhibitory activity of the complex (IC_{50} = 48.7 μM) did not markedly differ (Ψ = 0.9_{PA}) from its gallic acid precursor (IC_{50} = 45.2 μM), while both of them were less potent than acarbose (IC_{50} = 6.36 μM) by 7.7 (Ψ = 0.13_{AC}) and 7.1 (Ψ = 0.14_{AC}) folds, respectively (Figure 4b and Table 2). On the other hand, gallic acid, its Zn(II) complex and zinc acetate did not show dose response inhibition of in vitro BSA glycation compared with aminoguanidine (IC_{50} = 6.49 μM) (Figure 4c and Table 2).

The DPPH radical scavenging ability of the complex (IC_{50} = 8.79 μM) was significantly ($P < 0.05$) more active (Ψ = 5.5_{PA}) than its gallic acid precursor (IC_{50} = 48.2 μM) but did not differ significantly compared with ascorbic acid (IC_{50} = 9.98 μM) and Trolox (IC_{50} = 6.20 μM) (Figure 5a and Table 2). For ABTS radical scavenging activity, the Zn (II)-gallic acid complex (IC_{50} = 3.51 μM) outperformed gallic acid (IC_{50} = 12.7 μM; Ψ = 3.6_{PA}), ascorbic acid (IC_{50} = 47.1 μM; Ψ = 13.4_{AA}; $P < 0.05$), and Trolox (IC_{50} = 153 μM; Ψ = 43.6_{TR}; $P < 0.05$), while zinc acetate showed no radical scavenging activity (Figure 5b and Table 2). The Fe^{3+} reducing ability of the complex (1738 mmol/mol AAE) and its gallic precursor (1646 mmol/mol AAE) did not differ significantly from each other, but both showed significantly ($P < 0.05$)

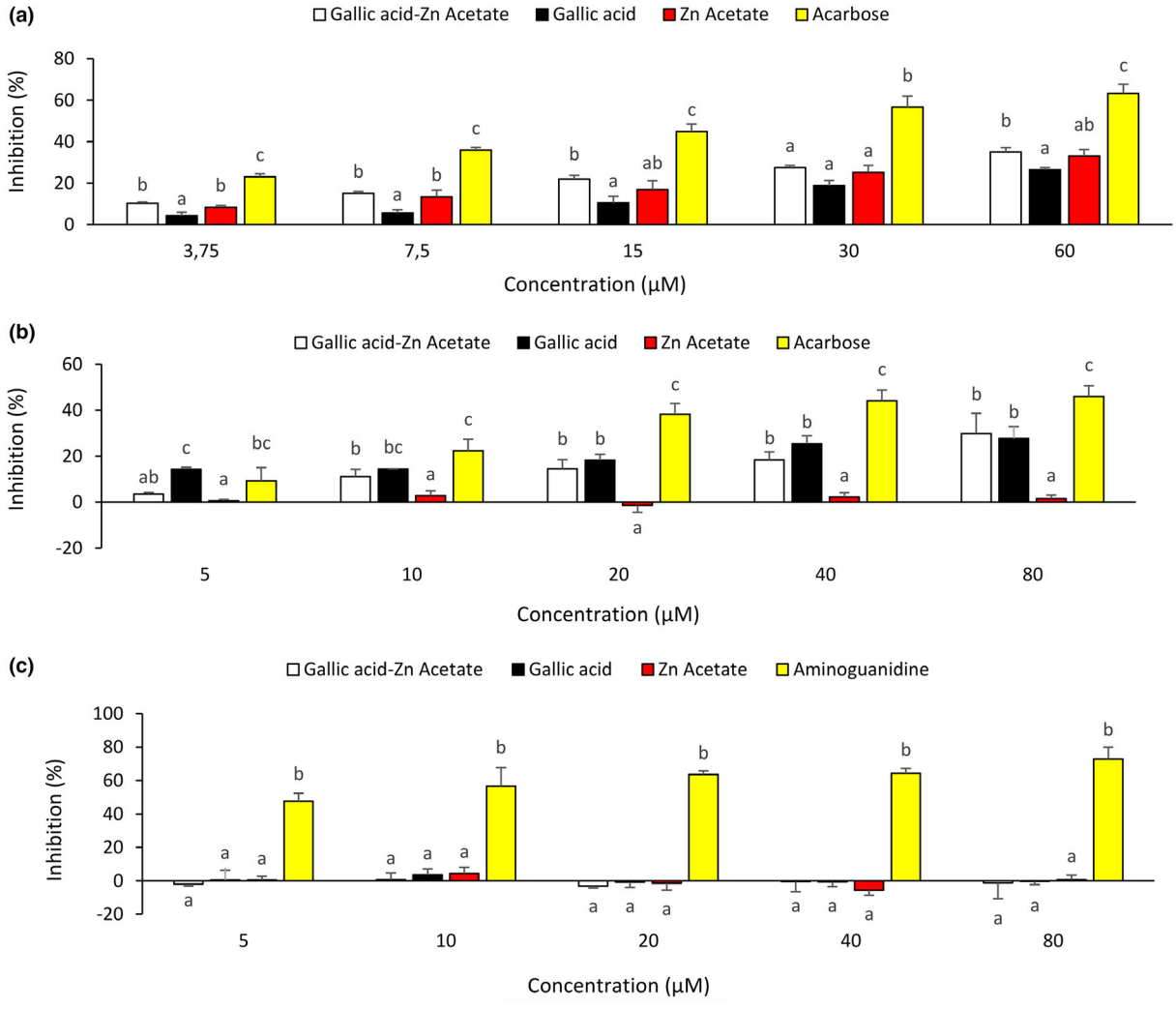

Figure 4 Effect of complex and precursors on (a) α-glucosidase, (b) α-amylase and (c) BSA glycation activities. Data are presented as mean ± SD of triplicate values. Different letters 'a', 'b' and 'c' mean that the value of one treatment group is significantly ($P < 0.05$) different from the other at a given concentration. [Colour figure can be viewed at wileyonlinelibrary.com]

Table 2 Summary table of the bioactivities of phenolic acid and complex (IC_{50} and EC_{50})

Parameters or activity	Gallic acid – Zn(II) complex	Gallic acid	Zn (II)	Ascorbic acid	Trolox	Acarbose	Aminoguanidine	Insulin
	IC_{50} or EC_{50} values (μM)							
ABTS radical scavenging activity (IC_{50})	3.51 ± 1.64^{c}	12.7 ± 4.39^{c}	ND	47.1 ± 4.47^{b}	153 ± 32.8^{a}	ND	ND	ND
DPPH radical scavenging activity (IC_{50})	8.79 ± 0.74^{b}	48.2 ± 5.43^{a}	ND	9.98 ± 2.04^{b}	6.20 ± 3.4^{b}	ND	ND	ND
Antiglycation activity (IC_{50})	ND	ND	ND	ND	ND	ND	6.49 ± 0.92^{c}	ND
α-amylase inhibition (IC_{50})	48.7 ± 7.10^{a}	45.2 ± 10.2^{a}	ND	ND	ND	6.36 ± 1.08^{b}	ND	ND
α-glucosidase inhibition (IC_{50})	21.5	58.5	39.8	ND	ND	9.08	ND	ND
L6-myotubes glucose uptake (EC_{50})	9.17	>10 000	208	ND	ND	ND	ND	ND

ND, not determined.

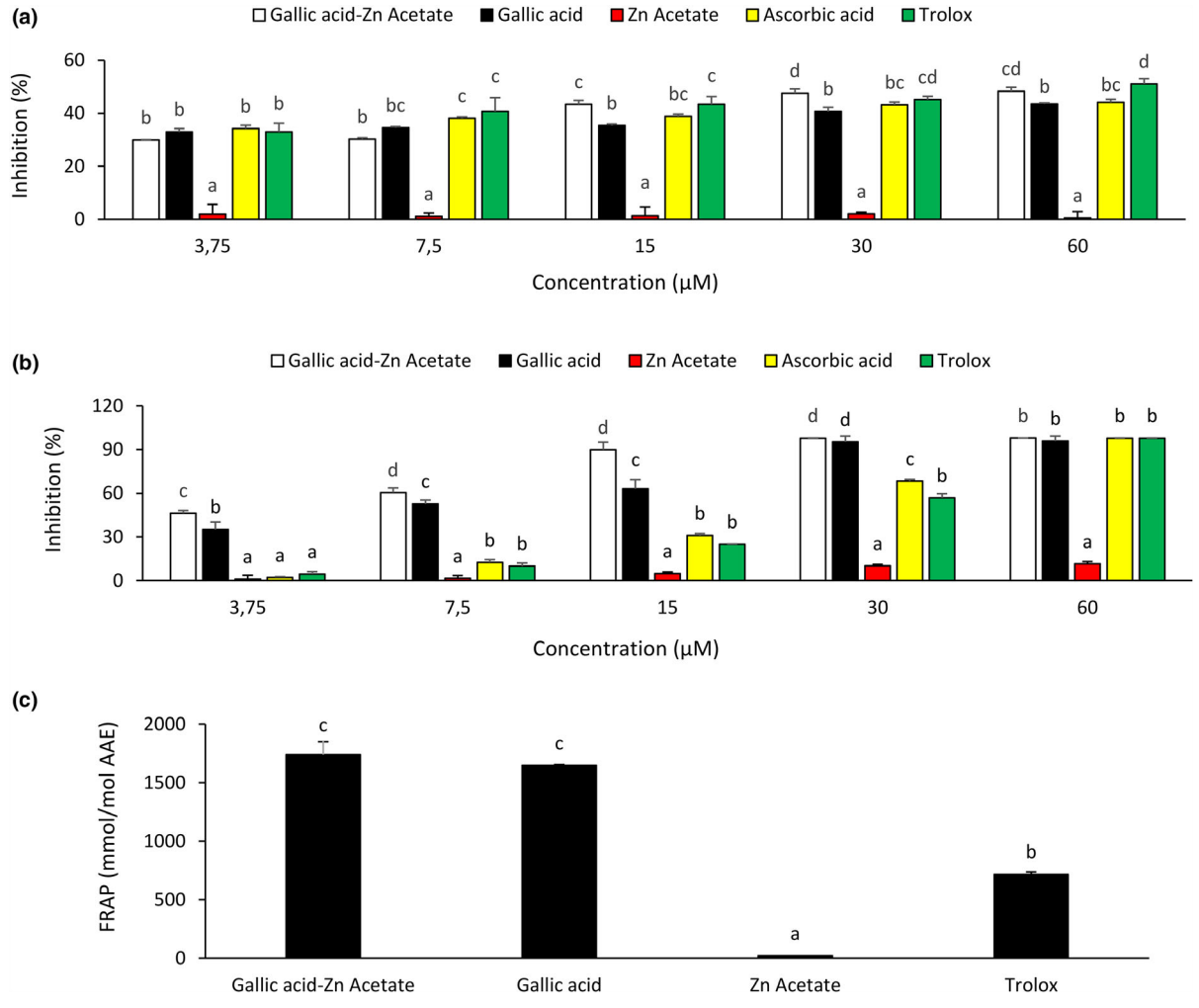

Figure 5 Effect of complex and precursors on (a) DPPH radical (b) ABTS radical and (c) Fe^{3+} ion. Data are presented as mean ± SD of triplicate values. Different letters 'a', 'b', 'c' and 'd' mean that the value of one treatment group is significantly ($P < 0.05$) different from the other at a given treatment concentration. [Colour figure can be viewed at wileyonlinelibrary.com]

stronger activities than Trolox (716 mmol/mol AAE) (Figure 5c).

Gallic acid dose-dependently but sparingly increased glucose uptake/utilization in differentiated L6 myotubes (EC_{50} = 3467 μg/ml or >10 000 μM) with 30% increase at the highest tested concentration (Figure 6a and Table 1). Both the complex (EC_{50} = 4.79 μg/ml ≡ 9.17 μM; $\Psi > 200_{PA}$) and Zn(II) (EC_{50} = 45.7 μg/ml ≡ 208 μM; $\Psi = 24_{PA}$) showed higher glucose uptake activity than gallic acid, while the activity of the complex was 22.7 folds that of Zn(II) acetate ($\Psi = 22.7_{ZA}$). However, both the complex (71% glucose uptake increase; $\Psi = 0.6_{IN}$) and Zn(II) acetate (63% glucose uptake increase; $\Psi = 0.5_{IN}$) were not as potent ($P < 0.05$) as a 1 μM insulin (133% glucose uptake increase) at the highest tested concentration (Figure 6a). The synthesized complex did not cause noticeable cytotoxicity in Chang liver cells and L6 myotubes at the tested concentrations (Figure 6c).

From the Ramachandran plot statistics, 96.43% of amino acid residues were plotted in favourable regions and only 1.1% residues were in the outer areas (Figure 7a). The model maintained stability and structural consistency for use in docking study (Figure 7a). The molecular docking study showed that the complex in the presence of two functionally active acetate moieties had higher docking scores than gallic acid (Table 3; Figure 7b and 7c). The docking scores of gallic acid were −4.66 and −4.38 kcal/mol, while that of the complex were −5.73 and −6.04 kcal/mol against the molecular targets, PKB and GLUT4, respectively (Table 3).

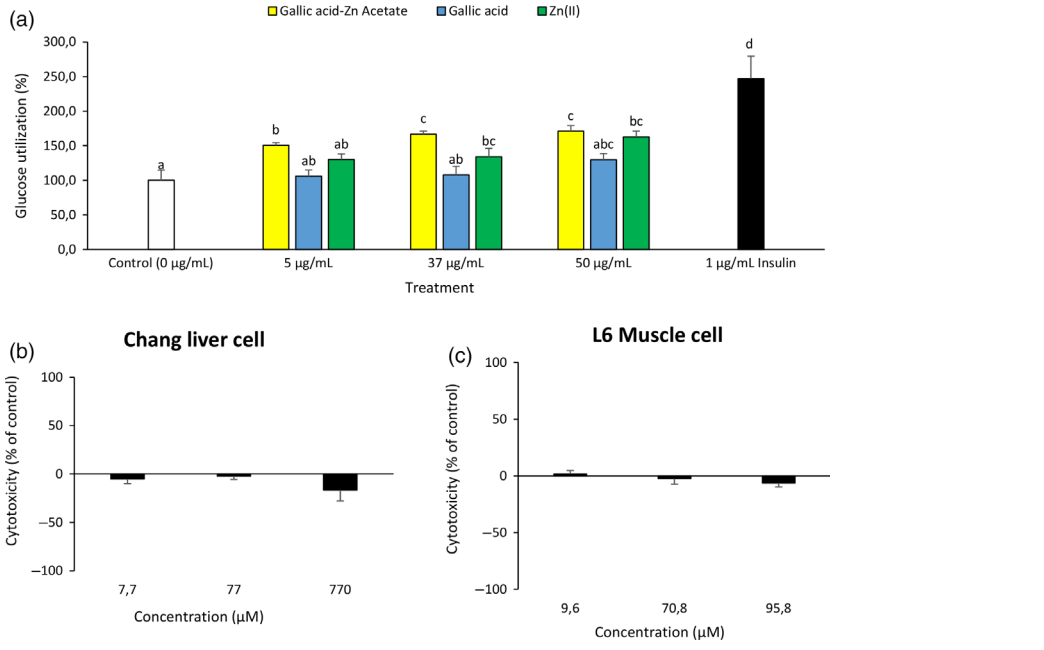

Figure 6 The effect of complex and precursors on (a) glucose uptake in differentiated L6 myotubes, (b) Chang liver cell viability, and (c) L6 myotube viability. Data are presented as mean ± SD of triplicate technical replicates to 2 biological repeats. Different letters 'a', 'b', 'c' and 'd' mean that the value of one treatment group is significantly ($P < 0.05$) different from the other at a given treatment concentration and when compared to the control and insulin treatments. [Colour figure can be viewed at wileyonlinelibrary.com]

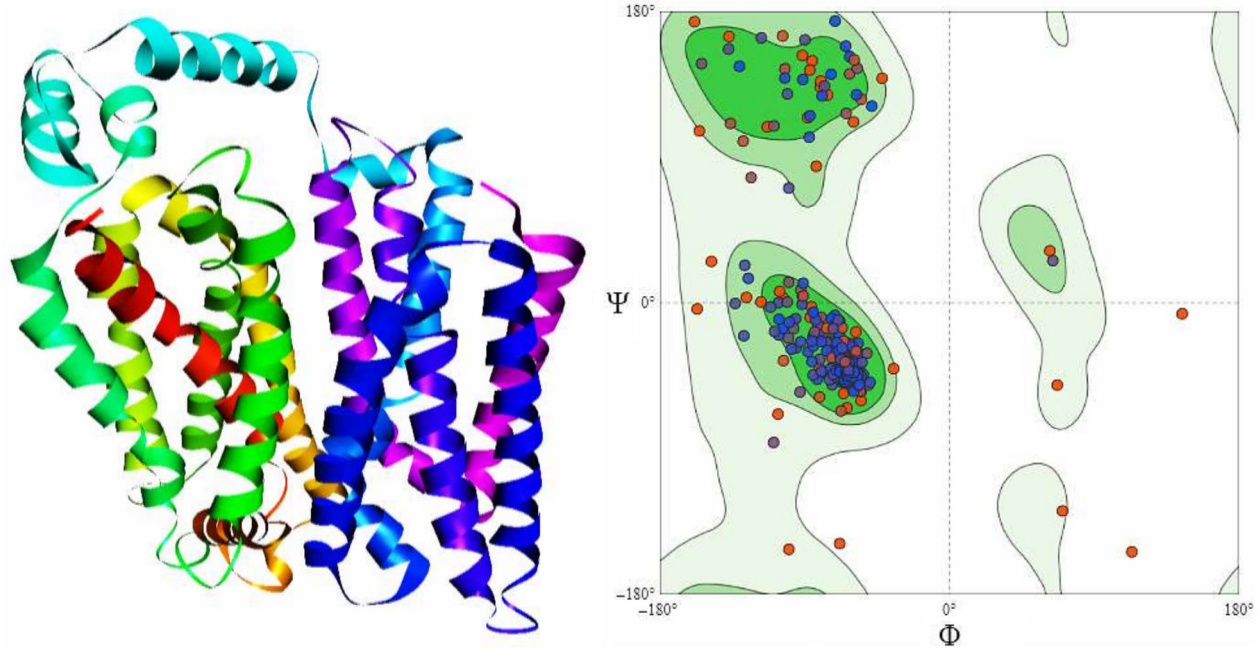

Figure 7 (a) Homology modelling and structural validation with the Ramachandran plot (96.43% residues in favourable and only 1.1 % residues were in outer regions) of human glucose transporter member 4 (GLUT-4) for docking study (b) Molecular interaction of (i) gallic acid and (ii) gallic acid-zinc acetate complex against the target GLUT4 (c) Molecular interaction of (i) gallic acid and (ii) gallic acid-zinc acetate complex against the target PKB. [Colour figure can be viewed at wileyonlinelibrary.com]

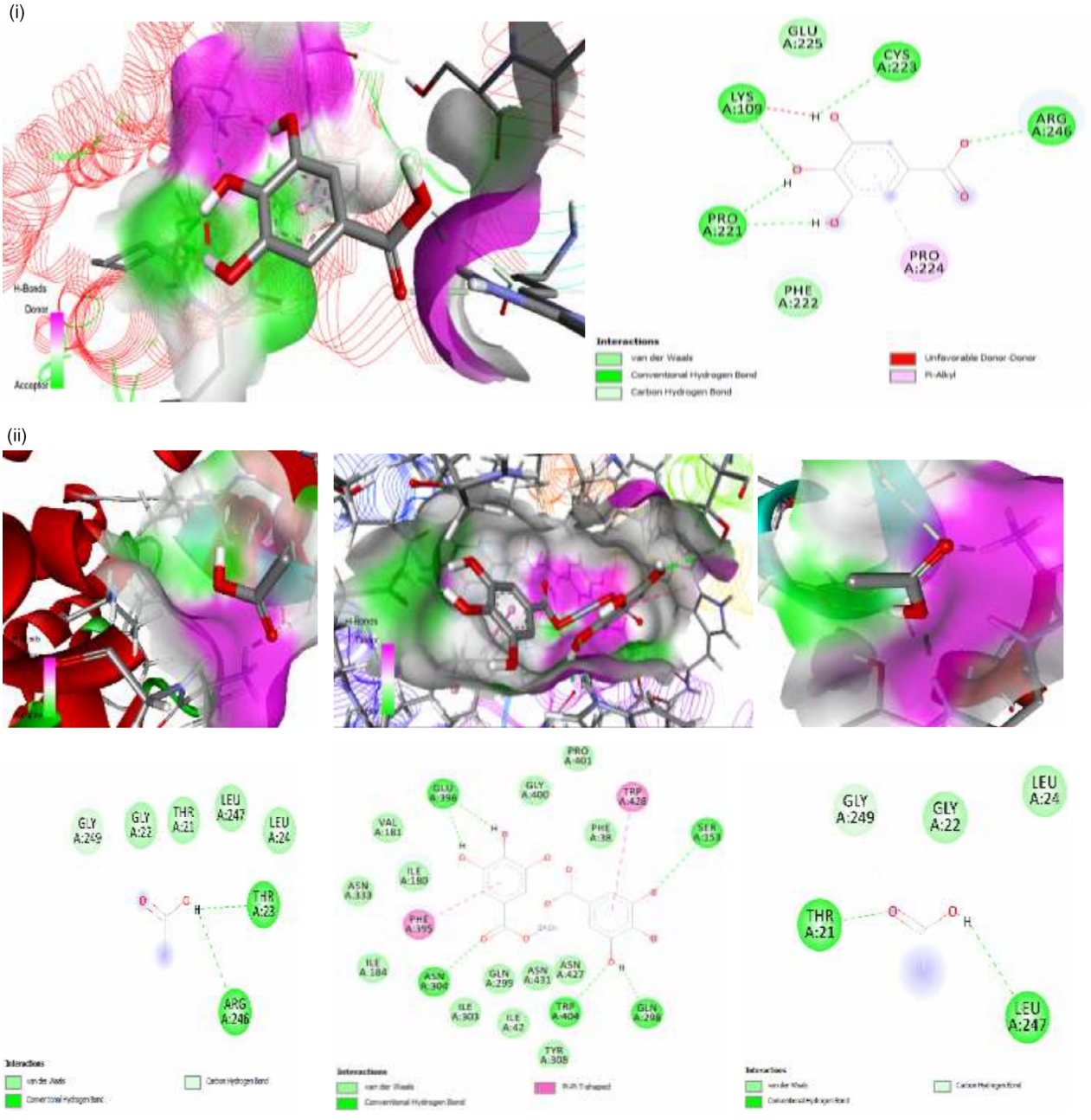

Figure 7 Continued

Discussion

The rich phytochemical profile of plants has been explored by man for many years in the management of several diseases, including diabetes. Gallic acid is one of the numerous plants-derived polyphenols with antioxidative and antidiabetic pharmacological credence.[15,38] On the other hand, the role of zinc in diabetes has been a subject of considerable interest, due to the insulin-mimetic properties associated with this mineral.[11] In this study, a novel Zn (II) complex of gallic acid was synthesized, with aim of developing an antidiabetic nutraceutical with, potentially, improved and multi-facet therapeutic action. Data showed that the synthesized complexed had two gallic acid moiety joint to Zn(II) by a $Zn(O_4)$ coordination and suggested a structure-activity relationship.

Amongst other outcomes, hyperglycaemia increases ROS and free radical production, which causes oxidative stress

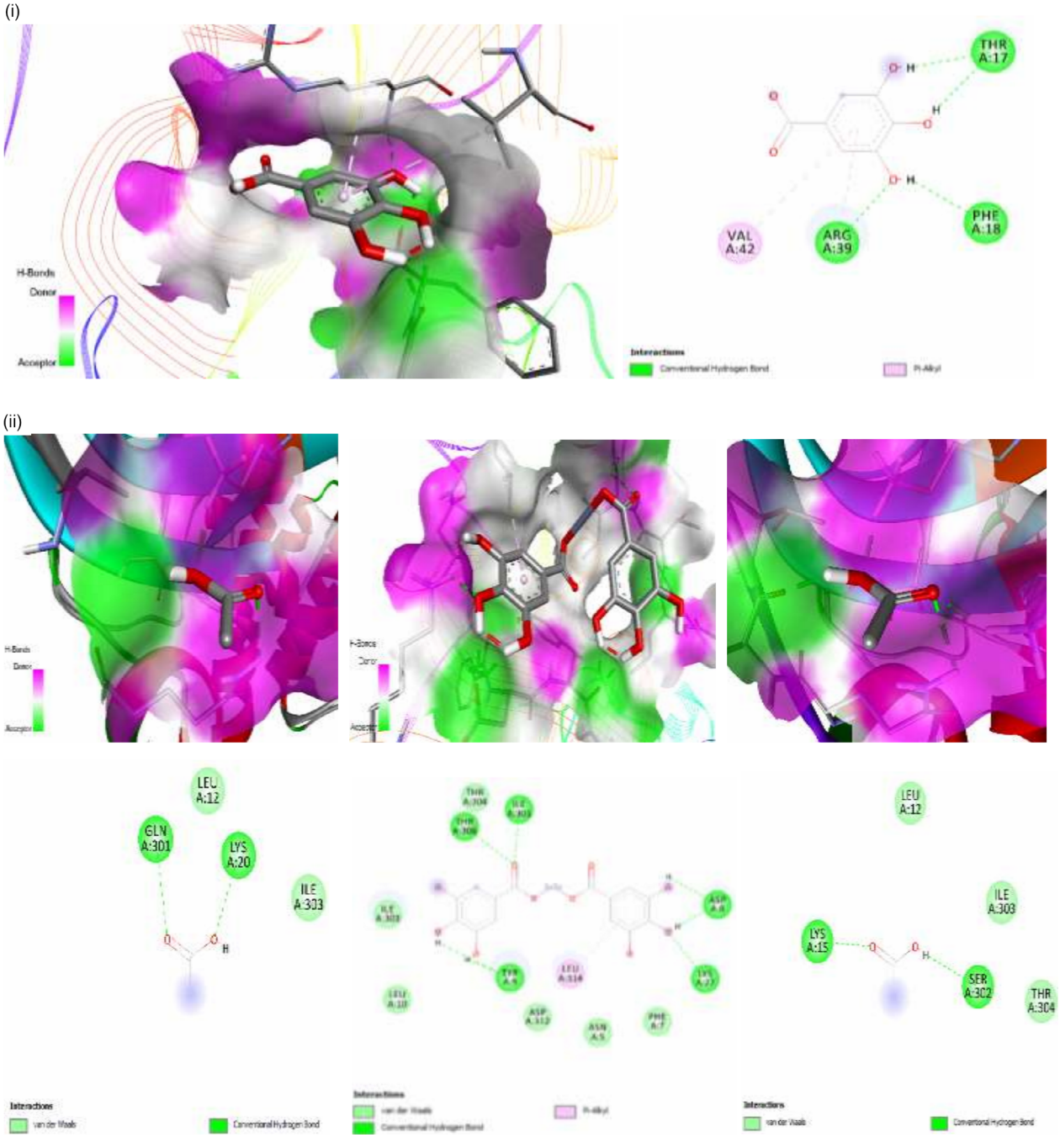

Figure 7 Continued.

and oxidative damage of biomolecules and organs, and subsequently, diabetic complications.[5] Polyphenols are known quenchers of free radical, because of their ability to form stable radical intermediates (phenoxy radical).[38] The previously reported radical scavenging ability of gallic acid[16] is consistent with its DPPH (IC_{50} = 48.2 μM) and ABTS (IC_{50} = 12.7 μM) radical scavenging and Fe^{3+} reducing (1646 mmol/mol AAE) activities observed in this study (Figure 5 and Table 2), which may be attributed to the phenolic polyhydroxy (-OH) groups present in gallic acid and its ability to form a phenoxy radical. Interestingly, the complex showed higher FRAP (1646 mmol/mol AAE) than gallic acid, while complexation dose-dependently increased ($P < 0.05$) the DPPH and ABTS radical

Table 3 Molecular docking score (Kcal/mol) of gallic acid and the Zn (II)-gallic acid metal complex against PKB and GLUT4

Selected target enzymes (PDB ID)	Gallic acid	Zn(II)-gallic acid metal complex
PKB (remodel of 106L)	−4.66	−5.75
GLUT-4 (homology model)	−4.38	−6.04

GLUT4, glucose transporter type 4; PDB, protein data bank; PKB, protein kinase B.

scavenging ability of gallic acid by 5.5 ($\Psi = 5.5_{PA}$) and 3.6 ($\Psi = 3.6_{PA}$) folds, respectively, exhibiting activities that were comparable to ascorbic acid and Trolox (Figure 5 and Table 2). Considering that Zn(II) acetate showed very poor antioxidant properties (Figure 5), the increased antioxidant property of the complex, relative its gallic acid precursor may be predominantly attributed to two gallic acid moieties acquired by the complex during complexation (Figure 1b).

Although not as potent as acarbose, the synthesized complex concomitantly and moderately inhibited carbohydrate digestive enzymes, α-glucosidase ($IC_{50} = 21.5$ μM) and α-amylase ($IC_{50} = 48.7$ μM) (Figures 4a and 4b and Table 2). These enzymes hydrolyse polysaccharide to release glucose, which is absorbed and contributes to postprandial glycaemia.[30] Thus, the inhibition of these enzymes by the complex suggests its potential as a postprandial glycaemic control agent. While Zn(II) complexation did not influence the α-amylase inhibitory effect of gallic acid ($\Psi \simeq 1_{PA}$), possibly because Zn(II) is a non-inhibitor of α-amylase, it increased its α-glucosidase inhibitory effect by 2.7 folds ($\Psi = 2.7_{PA}$) (Table 2). This effect of Zn(II) complexation on α-glucosidase inhibition may be partly attributed to the innate α-glucosidase inhibitory potential of Zn(II) acetate (Figure 4a and Table 2), which has been previously documented.[39] Additionally, gallic acid has been reported to have moderate inhibitory effect on α-glucosidase,[40] thus the 2 gallic acid moieties acquired by the complex during complexation (Figure 1b) may act synergistically with Zn (II) to improve the activity of the complex relative to gallic acid ($\Psi = 2.7_{PA}$) and Zn(II) acetate ($\Psi = 1.9_{ZA}$).

On the other hand, neither the complex, gallic nor Zn (II)acetate inhibited BSA glycation (Figure 4c and Table 2), suggesting that although the complex may modulate postprandial glycaemic control, it may not impede hyperglycaemia-induced glycation of biomolecules and formation of advanced glycation end-products.[41] Nevertheless, the excellent antioxidant and radical scavenging properties of the complex may be useful in ameliorating glycation-induced oxidative damage and diabetic complications.[41]

Amongst other mechanisms, insulin maintains glucose homeostasis by signalling the uptake and utilization of circulating glucose in cells of peripheral tissues, such as muscle cells and adipocytes.[4] In type 2 diabetic condition, these cells become non-responsive to insulin signalling, thus aggravating hyperglycaemia.[3] Insulin sensitizers like the thiazolidinediones are known antidiabetic drugs that improve insulin insensitivity in target tissues. Although gallic acid has been previously reported to induce GLUT-4 translocation and glucose uptake in adipocytes,[18] it only exerted mild dose-dependent glucose uptake in L6 myotubes by increasing glucose uptake by 30% at the highest tested concentration (Figure 6a and Table 2). On the other hand, the modulatory effects of Zn(II) on glucose uptake and related signalling factors have been well documented. Zn(II) stimulates the cyclic adenosine monophosphate (cAMP)-specific phosphodiesterase (PDE) activity, an enzyme that inactivates cAMP, and thus, downregulates cAMP-mediated lipolytic and glycogenolytic signalling.[10,42,43] In human and mouse skeletal muscle cells, Zn(II) modulated insulin signalling, which resulted in enhanced glucose oxidation and glycaemic control.[14] These reports are consistent with the observed dose-dependent modulatory effect ($EC_{50} = 208$ μM) of Zn(II) acetate on glucose uptake in L6 myotubes, which further significantly ($P < 0.05$) increased the activity of gallic acid by several folds ($EC_{50} = 9.17$ μM; $\Psi > 100_{PA}$) upon complexation (Figure 6a and Table 2). The glucose activity of the complex outperformed ($\Psi > 22.7_{ZA}$) that of Zn(II) acetate, suggesting that the two gallic acid moieties acquired by the complex (Figure 1b) may also influence or contribute to the improved bioactivity of the complex. Interestingly, toxicity evaluation showed that the complex did not cause toxicity in liver cells and myotubes (Figure 6b and 6c). Data suggest that the synthesized complex may control glycaemia without possible toxicity concerns.

Previous studies suggest that the modulatory effect of Zn (II) or its complex on insulin signalling may be linked to phosphorylation of adenosine monophosphate-activated protein kinase and insulin receptor sub-unit; activation of PKB (Akt) signalling pathway; and increase of GLUT-4 expression and translocation, which will, collectively, promote glucose uptake in skeletal muscle cells and adipocytes.[11] Molecular docking analysis showed that Zn(II) complexation resulted in increased interaction with molecular targets (PKB and GLUT-4) of the insulin signalling (Figure 7b and 7c), which suggests that Zn(II) and its complex may modulate glucose uptake in L6 myotubes through the above-mentioned mechanisms.

Conclusion

The complexation between Zn(II) acetate and gallic acid ligand appeared as a $Zn(O_4)$ coordination mode, thus the complex acquired two gallic acid molecules. This attribute seemed influential in the ability for complexation to improve some of the pharmacological properties of gallic

acid by several folds. Additionally, Zn(II) conferred a potent insulin-mimetic (glucose uptake) property on gallic acid resulting in a complex with multimode antioxidant, enzyme inhibitory and glucose uptake modulatory potentials. This study suggests that the synthesized complex may be further studied as a safe and multimode acting antioxidant and glycaemic control nutraceutical for T2D and oxidative complications.

Declarations

Conflict of interest

The authors declare that there is no conflict of interest with this work.

Funding

This work was supported by the following: (i) South African National Research Foundation (NRF) under the Freestanding Postdoctoral Fellowship Scholarship (Grant reference number: 116701) and (ii) The Postgraduate Research office of the Central University of Technology, Bloemfontein under the postdoctoral research funding.

Authors' contributions

Chika I. Chukwuma conceptualized and designed the study. Denice M. Motloung and Godfery R Matowane carried out the synthesis and in vitro antidiabetic and antioxdative evaluation of the complex under the main supervision and co-supervision of Chika I. Chukwuma and Samson S. Mashele, respectively. Denice M. Motloung prepared the initial draft of manuscript, while Chika I. Chukwuma and Samson S. Mashele made revision on the final version. Chika I. Chukwuma and Samson S. Mashele did the FITR, glucose uptake and cytotoxicity study and the data interpretation. Shasank S. Swain did the molecular docking study and data interpretation. Susanna L. Bonnet and Anwar E.M. Noreljaleel did the NMR study and the data interpretation. Sunday O. Oyedemi was partly involved in the FITR study and revising initial draft of manuscript. Shasank S. Swain, Susanna L. Bonnet and Anwar E.M. Noreljaleel, also, proof-read the final version of manuscript and made necessary inputs.

References

1. American Diabetes Association. Diagnosis and classification of diabetes mellitus. *Diabetes Care* 2014; 37(Supp. 1): S81–S90. https://doi.org/10.2337/dc14-S081
2. International Diabetes Federation (IDF). *IDF Diabetes Atlas*, 8th edn, 2017. http://diabetesatlas.org/resources/2017-atlas.html (accessed 13 April 2018).
3. Wu Y *et al*. Risk factors contributing to type 2 diabetes and recent advances in the treatment and prevention. *Int J Med Sci* 2014; 11: 1185–2000.
4. Aronoff SL *et al*. Glucose metabolism and regulation: beyond insulin and glucagon. *Diabetes Spectr* 2004; 17: 183–190.
5. Pourghassem-Gargari B *et al*. Effect of supplementation with grape seed (*Vitis vinifera*) extract on antioxidant status and lipid peroxidation in patient with type II diabetes. *J Med Plants Res* 2011; 5: 2029–2034.
6. Chukwuma CI *et al*. A comparative study on the physicochemical, antioxidative, anti-hyperglycemic and anti-lipidemic properties of amadumbe (*Colocasia esculenta*) and okra (*Abelmoschus esculentus*) mucilage. *J Food Biochem* 2018; 42: e12601. https://doi.org/10.1111/jfbc.12601.
7. Kibiti CM, Afolayan AJ. The biochemical role of macro and micro-minerals in the management of diabetes mellitus and its associated complications: a review. *Int J Vitam Nutr Res* 2015; 85: 88–103.
8. Kimball SM *et al*. Effect of a vitamin and mineral supplementation on glycemic status: Results from a community-based program. *J Clin Transl Endocrinol* 2017; 10: 28–35.
9. Mooradian AD *et al*. Selected vitamins and minerals in diabetes. *Diabetes Care* 1994; 17: 464–479.
10. Adachi Y *et al*. A new insulin-mimetic bis (allixinato) zinc (II) complex: structure–activity relationship of zinc (II) complexes. *J Biol Inorg Chem* 2004; 9: 885–893.
11. Chukwuma CI *et al*. A comprehensive review on zinc(II) complexes as antidiabetic agents: the advances, scientific gaps and prospects. *Pharmacol Res* 2020a; 155: 104744. https://doi.org/10.1016/j.phrs.2020.104744.
12. Ezaki O. IIb group metal ions (Zn^{2+}, Cd^{2+}, Hg^{2+}) stimulate glucose transport activity by post-insulin receptor kinase mechanism in rat adipocytes. *J Biol Chem* 1989; 264: 16118–16122.
13. Shisheva A *et al*. Insulin-like effects of zinc ion in vitro and in vivo: preferential effects on desensitized adipocytes and induction of normoglycemia in streptozocin-induced rats. *Diabetes* 1992; 41: 982–988.
14. Norouzi S *et al*. Zinc stimulates glucose oxidation and glycemic control by modulating the insulin signaling pathway in human and mouse skeletal muscle cell lines. *PLoS One* 2018; 13: e0191727. https://doi.org/10.1371/journal.pone.0191727.
15. Vinayagam R *et al*. Anti-diabetic effects of simple phenolic acids: a comprehensive review. *Phytother Res* 2016; 30: 184–199.
16. Reckziegel P *et al*. Antioxidant protection of gallic acid against toxicity induced by Pb in blood, liver and kidney of rats. *Toxicol Rep* 2016; 3: 351–356.

17. Aryaneian N *et al*. Polyphenols and their effects on diabetes management: a review. *Med J Islam Repub Iran* 2017; 31: 134. https://doi.org/10.14196/mjiri.31.134.
18. Variya BC *et al*. Antidiabetic potential of gallic acid from *Emblica officinalis*: improved glucose transporters and insulin sensitivity through PPAR-γ and Akt signaling. *Phytomedicine* 2019; 152906: https://doi.org/10.1016/j.phymed.2019.152906.
19. Adefegha SA *et al*. Antioxidant and antidiabetic effects of gallic and protocatechuic acids: a structure–function perspective. *Comp Clin Path* 2015; 24: 1579–1585.
20. Patel SS, Goyal RK. Cardioprotective effects of gallic acid in diabetes-induced myocardial dysfunction in rats. *Pharmacognosy Res* 2011; 3: 239–245.
21. Vijayaraghavan K *et al*. Design, synthesis and characterization of zinc-3 hydroxy flavone, a novel zinc metallo complex for the treatment of experimental diabetes in rats. *Eur J Pharmacol* 2012; 680: 122–129.
22. Sendrayaperumal V *et al*. Design, synthesis and characterization of zinc–-morin, a metal flavonol complex and evaluation of its antidiabetic potential in HFD–STZ induced type 2 diabetes in rats. *Chem Biol Interact* 2014; 219: 9–17.
23. Gopalakrishnan V *et al*. Synthesis, spectral characterization, and biochemical evaluation of antidiabetic properties of a new zinc-diosmin complex studied in high fat diet fed-low dose streptozotocin induced experimental type 2 diabetes in rats. *Biochem Res Int* 2015; 2015: 350829. https://doi.org/10.1155/2015/350829.
24. Al-Ali K *et al*. Dual effect of curcumin–zinc complex in controlling diabetes mellitus in experimentally induced diabetic rats. *Biol Pharm Bull* 2016; 39: 1774–1780.
25. Kozlevčar B *et al*. Complexes with lignin model compound vanillic acid. Two different carboxylate ligands in the same dinuclear tetracarboxylate complex [Cu2 (C8H7O4) 2 (O2CCH3) 2 (CH3OH) 2]. *Polyhedron* 2006; 25: 1161–1166.
26. Sanni O *et al*. *Azadirachta indica* inhibits key enzyme linked to type 2 diabetes in vitro, abates oxidative hepatic injury and enhances muscle glucose uptake ex vivo. *Biomed Pharmacother* 2019; 109: 734–743.
27. Re R *et al*. Antioxidant activity applying an improved ABTS radical cation decolorization assay. *Free Radic Biol Med* 1999; 26: 1231–1237.
28. Oyedemi SO *et al*. Alpha-amylase inhibition and antioxidative capacity of some antidiabetic plants used by the traditional healers in Southeastern Nigeria. *Sci World J* 2017; 2017: 3592491. https://doi.org/10.1155/2017/3592491.
29. Nakagawa T *et al*. Protective activity of green tea against free radical-and glucose-mediated protein damage. *J Agric Food Chem* 2002; 50: 2418–2422.
30. Chukwuma CI *et al*. Evaluation of the in vitro -amylase inhibitory, antiglycation, and antioxidant properties of *Punica granatum* L. (pomegranate) fruit peel acetone extract and its effect on glucose uptake and oxidative stress in hepatocytes. *J Food Biochem* 2020b; 44: e13175. https://doi.org/10.1111/jfbc.13175.
31. Van Huyssteen M *et al*. Antidiabetic and cytotoxicity screening of five medicinal plants used by traditional African health practitioners in the Nelson Mandela Metropole, South Africa. *Afr J Tradit Complement Altern Med* 2011; 8: 150–158.
32. Oyedemi S *et al*. *In vitro* anti-hyperglycemia properties of the aqueous stem bark extract from *Strychnos henningsii* (Gilg). *Int J Diabetes Dev C* 2013; 33: 120–127.
33. Swain SS *et al*. Molecular docking and simulation study for synthesis of alternative dapsone derivative as a newer anti-leprosy drug in multidrug therapy. *J Cell Biochem* 2018; 119: 9838–9852.
34. Swain SS *et al*. Synthesis of novel thymol derivatives against MRSA and ESBL producing pathogenic bacteria. *Nat Prod Res* 2019; 33: 3181–3189.
35. Hirun N *et al*. Experimental FTIR and theoretical studies of gallic acid–acetonitrile clusters. *Spectrochim Acta A Mol Biomol Spectrosc* 2012; 86: 93–100.
36. Oliveira RN *et al*. FTIR analysis and quantification of phenols and flavonoids of five commercially available plants extracts used in wound healing. *Matéria (Rio de Janeiro)* 2016; 21: 767–779.
37. Hasana H, Desalegn E. Characterization and quantification of phenolic compounds from leaf of *Agarista salicifolia*. *Herb Med* 2017; 3: 2. https://doi.org/10.21767/2472-0151.100022 .
38. Shahidi F, Wanasundara PD. Phenolic antioxidants. *Crit Rev Food Sci Nutr* 1992; 32: 67–103.
39. Miyazaki R *et al*. α-Glucosidase inhibition by new Schiff base complexes of Zn (II). *Open J Inorgc Chem* 2016; 6: 114–124.
40. Everette JD *et al*. Inhibitory activity of naturally occurring compounds towards rat intestinal α-glucosidase using p-nitrophenyl-α-d-glucopyranoside (PNP-G) as a substrate. *Am J Food Technol* 2013; 8: 65–73.
41. Cooper ME. Importance of advanced glycation end products in diabetes-associated cardiovascular and renal disease. *Am J Hypertens* 2004; 17: 31S–38S.
42. Percival MD *et al*. Zinc dependent activation of cAMP-specific phosphodiesterase (PDE4A). *Biochem Biophys Research Comm* 1997; 241: 175–180.
43. Yoshikawa Y *et al*. The action mechanism of zinc (II) complexes with insulinomimetic activity in rat adipocytes. *Life Sci* 2004; 75: 741–751.